Electronic Supplementary Material (ESI) for Materials Chemistry Frontiers.
This journal is © the Partner Organisations 2022

Supporting Information for

Single atom substitution in donor-acceptor covalent organic frameworks for tunable visible light photocatalytic Cr(VI) reduction

Jie-Yu Yue,‡ Yu-Tong Wang,‡ Xiu-Li Ding, Yan-Fei Fan, Li-Ping Song, Peng Yang, Yu Ma* and Bo Tang*

College of Chemistry, Chemical Engineering and Materials Science, Collaborative Innovation Center of Functionalized Probes for Chemical Imaging in Universities of Shandong, Key Laboratory of Molecular and Nano Probes, Ministry of Education, Institutes of Biomedical Sciences, Shandong Normal University, Jinan, 250014, P. R. China.

Corresponding Author: Dr. Yu Ma and Bo Tang

*E-mail: may@sdnu.edu.cn; tangb@sdnu.edu.cn

‡These authors contributed equally to this work.

1. Supplementary materials

1.1. Materials

1,3,6,8-tetrakis(4-formylphenyl)pyrene (TFPPY) was purchased from Jilin Chinese Academy of Sciences Yanshen Technology Co., Ltd. $Pd(PPh_3)_4$, $K_2Cr_2O_7$, 1,5-diphenylcarbonohydrazide, terephthalic acid (TA), $AgNO_3$, 1,4-benzoquinone (PBQ), KI, triacetonediamine (TEMP), isopropyl alcohol (IPA), ferrocene, tetrabutylammonium hexafluorophosphate, 2,2,6,6-tetramethylpiperidinyloxy (TEMPO) and Nitrotetrazolium blue chloride (NBT) were purchased from Energy Chemical. 4,7-dibromo-2,1,3-benzothiadiazole and 4-(4,4,5,5-Tetramethyl-1,3,2-dioxaborolan-2-yl)aniline were booked from Bide Pharmaceutical Technology Co., Ltd. The H_2O_2 Detection Kit (titanium sulfate colorimetric method) purchased from Leagene Biotechnology. All the chemicals involved in this work were utilized with no further purification.

1.2. Instruments

The powder X-ray diffraction (PXRD) characterization was carried out on D8 ADVANCE with Cu Kα radiation (λ = 1.5405 Å) with a 2θ range from 2° to 30° at room temperature. The Brunauer-Emmett-Teller (BET) surface areas were tested on an ASAP 2020/TriStar 3000 (Micromeritics) at 77 K. ^{1}H NMR spectra were performed on Bruker Avance 400 MHz NMR spectrometers. Fourier transform infrared (FT-IR) Spectra were acquired on Bruker ALPHA FT-IR Spectrometer ranging from 500 to 4000 cm^{-1}. Solid-state ^{13}C NMR spectrum was exploited on a Bruker Avance III 400 MHz instrument. Scanning electron microscopy (SEM) images were conducted on a SUB010 instrument. Transmission electron microscopy (TEM) images were collected on Hitachi HT7700 electron microscope. Thermogravimetric analysis (TGA) was performed on TGA/SDTA851e in N_2 atmosphere at 10 °C min^{-1} from 30 °C to 900 °C. The Ultraviolet-visible (UV-Vis) spectra were collected on a Hitachi U-4100 spectrophotometer. Fluorescence spectra were collected on with F-4600 FL Spectrophotometer (Hitachi, Japan). X-ray photoelectron spectroscopy (XPS) spectra were obtained from PHI Versaprobe II. Photoreduction experiments were performed on a NAI-GHY-DSGKW instrument and illuminated by a 300 W Xe lamp with a cut-off filter ($\lambda \geq 400$ nm). Electrochemical tests were performed on electrochemical workstation (Chenhua, China, CHI 660E). Electron spin resonance (ESR) spectra were recorded on a Bruker A300-10/12 instrument.

2. Supplementary experimental details

2.1. Synthesis of 4,4′-(benzoselenadiazole-4,7-diyl)dibenzaldehyde (SEZ)

4,7-dibromo-2,1,3-benzoselenodiazole (500 mg, 1.46 mmol),[1] 4-(4,4,5,5-Tetramethyl-1,3,2-dioxaborolan-2-yl)aniline (865 mg, 4.29 mmol), $Pd(PPh_3)_4$ (200 mg) and sodium carbonate (1.27 g) were put into a 100 mL round bottom flask. 40 mL of dioxane and 10 mL of water were added as solvents and the mixed system was heated to reflux at 110 °C in N_2 atmosphere for 48 h. After the reaction was completed, 50 mL of water was added into the system. The crude product was extract with dichloromethane (DCM) and purified by silica gel column with petroleum ether and ethyl acetate (1/2) as eluent and finally a dark red solid with yield about 60% was obtained. ^{1}H NMR (400 MHz, DMSO-d_6), δ (ppm) = 7.68 (d, J = 8.5 Hz, 4H), 7.52 (s, 2H), 6.68 (d, J = 8.5 Hz, 4H), 5.31 (s, 4H).

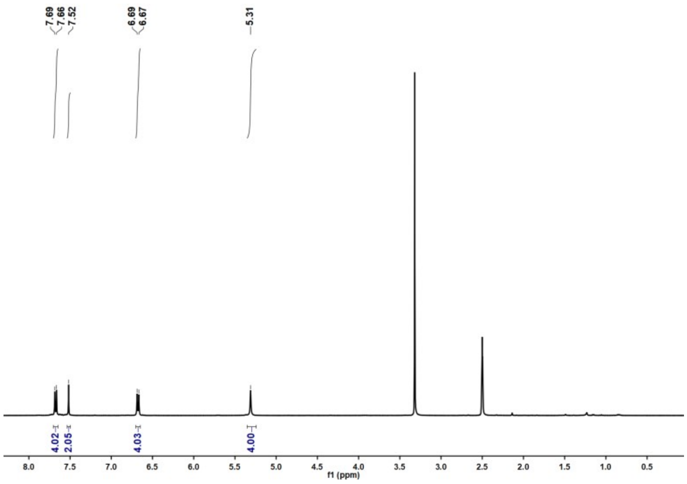

2.2. Synthesis of 4,4′-(benzothiadiazole-4,7-diyl)dibenzaldehyde (BTZ)

BTZ was synthesized according to the previous literature.[2] Briefly, 4,7-dibromo-2,1,3-benzothiadiazole (835 mg, 2.84 mmol), 4-(4,4,5,5-Tetramethyl-1,3,2-dioxaborolan-2-yl)aniline (1.5 g, 7.43 mmol), Pd(PPh_3)$_4$ (115 mg) and sodium carbonate (1.9 g) were put into a 100 mL round bottom flask. 50 mL of dioxane and 10 mL of water were added as solvents and the mixed system was heated to reflux at 110 °C in N_2 atmosphere for 48 h. After the reaction was completed, 50 mL of water was added into the system. The crude product was extract with dichloromethane (DCM) and purified by silica gel column with petroleum ether and ethyl acetate (1/2) as eluent and finally a dark red solid with yield about 75% was obtained. ^{1}H NMR (400 MHz, DMSO-d_6): δ (ppm) = 7.76 (d, J = 8.5 Hz, 4H), 7.73 (s, 2H), 6.71 (d, J = 8.5 Hz, 4H), 5.37 (s, 4H).

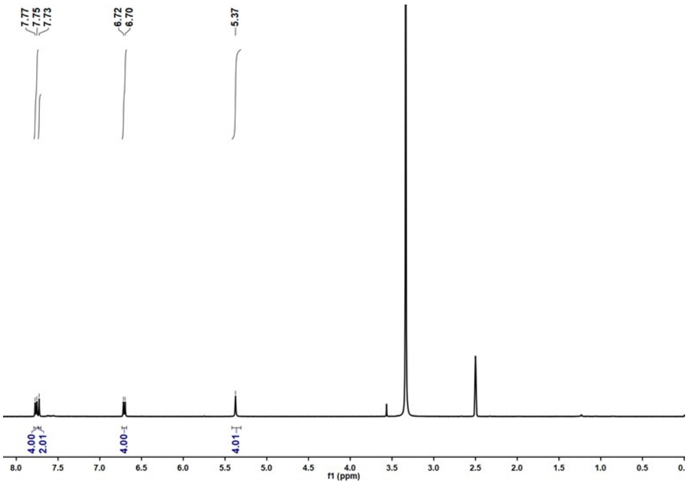

2.3. Cyclic voltammetry (CV) measurements

2 mg of COF (PYE-COF and PYS-COF, respectively), 1 mg of acetylene black and

20 μL of Nafion solution (5 wt%) were dispersed in 1 mL of ethanol and sonicated for 30 min to get a well dispersed black ink. Then 10 μL of ink was loaded on the pre-polished glass carbon electrode (diameter: 3 mm) as the working electrode. The Ag/AgCl (KCl-saturated) electrode was utilized as the reference electrode and the platinum wire was served as the counter electrode. Anhydrous acetonitrile with tetrabutylammonium hexafluorophosphate (0.1 M) was applied as electrolyte solution. CV curves were collected with a scan rate of 100 mV s^{-1}. The experimental results were calibrated by the standard ferrocene/ferrocenium (Fc) redox system.

2.4. Photocurrent measurements

COF (PYE-COF and PYS-COF, respectively) coated FTO (1 × 2 cm^2) was served as the working electrode, Ag/AgCl (KCl-saturated) electrode was utilized as the reference electrode and the platinum plate was served as the counter electrode. Na_2SO_4 solution (0.5 M) was utilized as electrolyte. A 300 W Xe lamp (CEL-HXF300) ($\lambda \geq 400$ nm) was served as the light source.

2.5. ESR test

200 μL of PYE-COF dispersions (1 mg/mL, water as solvent) and 100 μL of TEMPO solution (5 mM) were mixed and sonicated. The mixture was transferred into the quartz tube and then ESR spectrum was collected immediately. After irradiation under a 300 W Xe lamp (CEL-HXF300) ($\lambda \geq 400$ nm) for 5 min, ESR spectrum was recollected.

2.6. Detection of superoxide radical by NBT

2 mg of PYE-COF and 10 mL of NBT solution (0.025 mM) were mixed and dispersed in a quartz tube. The quartz tube was illuminated by a 300 W Xe lamp with a cut-off filter ($\lambda \geq 400$ nm) and cooled by circulating water. After irradiation at different times (0 min, 30 min, 60 min, and 90 min, respectively), the supernatant was collected by centrifugation and the UV-Vis spectra were collected.

2.7. Detection of hydroxyl radical by TA

5 mg of PYE-COF and 8 mL of TA solution (5 mM, NaOH aqueous solution as solvent) were mixed in a quartz tube, sonicated and subsequently stirred in the dark for 10 min. The quartz tube was illuminated by a 300 W Xe lamp with a cut-off filter

($\lambda \geq 400$ nm) and cooled by circulating water. After irradiation at different times (0 min, 5 min, 10 min, and 20 min, respectively), the supernatant was collected by centrifugation. The fluorescent spectra of the supernatant at 426 nm were recorded excited at 320 nm.

2.8. Reactive species quenching experiments

Different scavengers were added into the reduction systems. Typically, 0.1 mM of $AgNO_3$, PBQ, KI, TEMP and IPA were introduced into the reaction quartz tubes to quench the electron, $O_2^{\bullet-}$, hole, $^1O_2$ and •OH, respectively. After irradiation for 40 min, the Cr(VI) reduction efficiency were checked.

3. Supplementary figures and tables

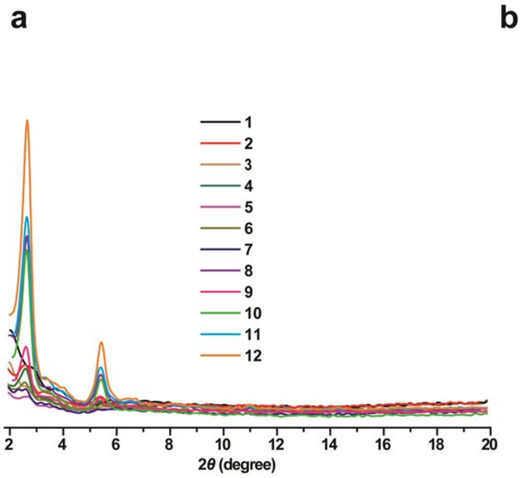

b

	solvent
1	*o*-DCB 0.5 mL; EtOH 0.5 mL
2	*o*-DCB 0.75 mL; EtOH 0.25 mL
3	*o*-DCB 0.25 mL; EtOH 0.75 mL
4	*o*-DCB 0.5 mL; *n*-BuOH 0.5 mL
5	*o*-DCB 0.75 mL; *n*-BuOH 0.25 mL
6	*o*-DCB 0.25 mL; *n*-BuOH 0.75 mL
7	*o*-DCB 0.3 mL; EtOH 0.7 mL
8	o-DCB 0.9 mL; *n*-BuOH 0.1 mL
9	*o*-DCB 0.9 mL; CH_3OH 0.1 mL
10	*o*-DCB 0.9 mL; Dioxane 0.1 mL
11	*o*-DCB 0.9 mL; Mesitylene 0.1 mL
12	***o*-DCB 0.9 mL; EtOH 0.1 mL**

Fig. S1 Synthesis conditions of PYE-COF.

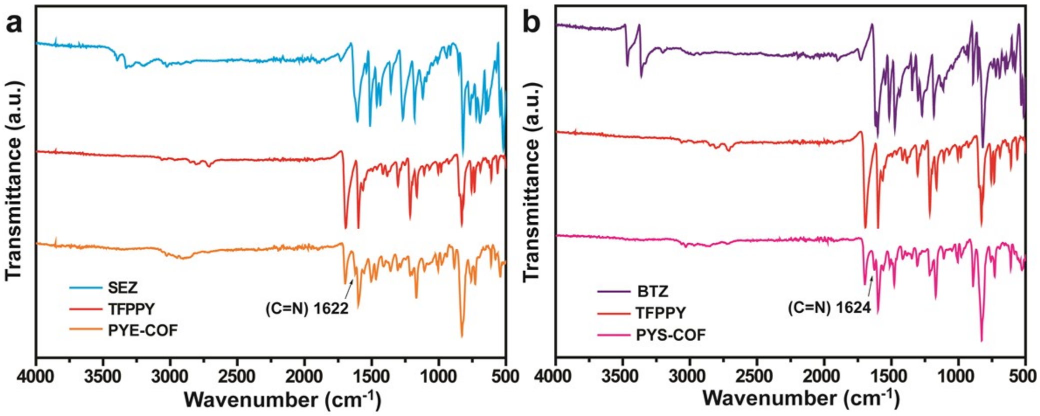

Fig. S2 The FT-IR spectra of (a) PYE-COF and (b) PYS-COF.

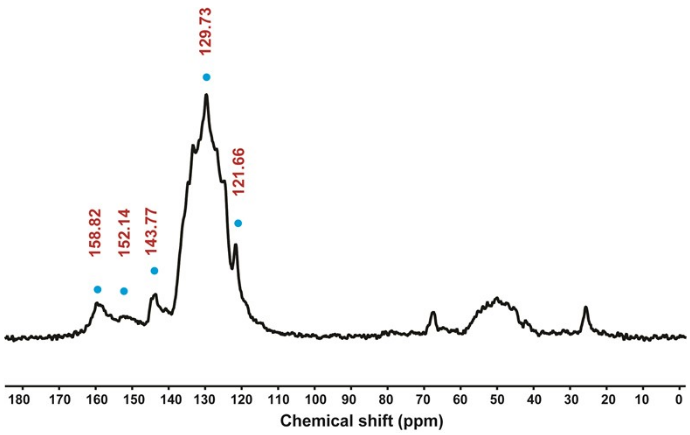

Fig. S3 The solid-state ^{13}C NMR spectrum of PYE-COF.

Fig. S4 SEM images of (a) PYE-COF and (b) PYS-COF; TEM images of (c) PYE-COF and (d) PYS-COF.

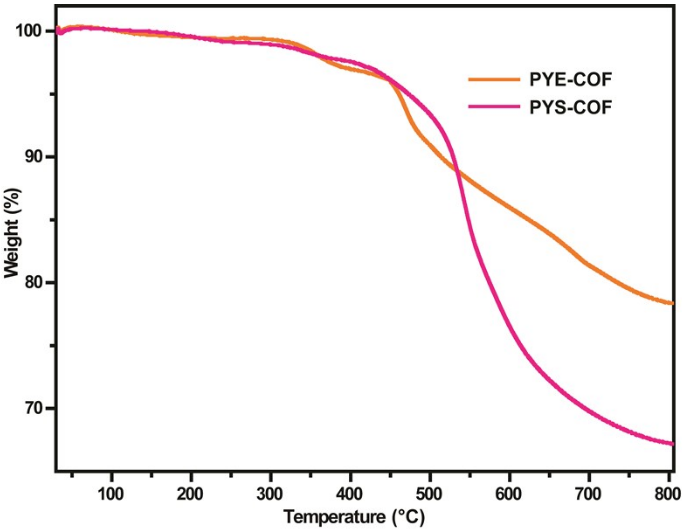

Fig. S5 TGA curves of PYE-COF and PYS-COF.

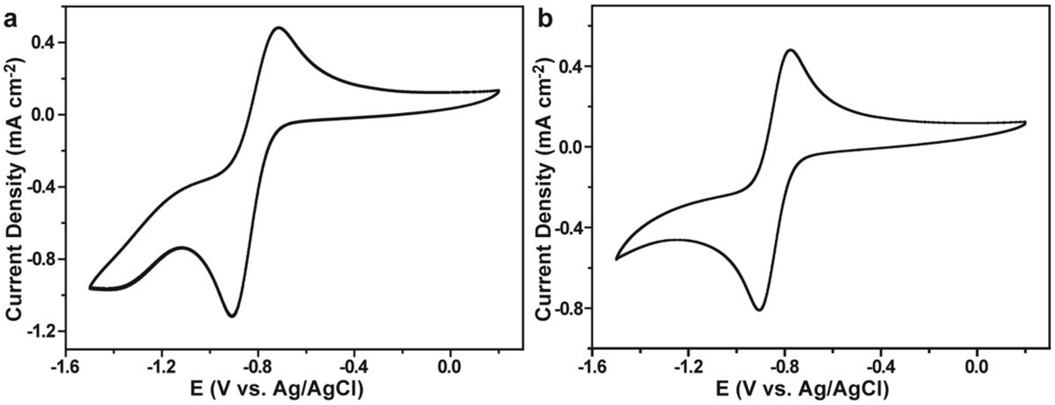

Fig. S6 CV curves of (a) PYE-COF and (b) PYS-COF utilizing Fc as an internal standard with a scan rate of 100 mV s^{-1}. The relative E_{HOMO} and E_{LUMO} are calculated according to the following equation:[3] (1) $E_{\mathrm{LUMO}} = -\,[E_{\mathrm{red}}\,(\mathrm{onset}) - E_{1/2}\,(\mathrm{Fc}) + 4.8]$ eV ; (2) $E_{\mathrm{g}} = E_{\mathrm{LUMO}} - E_{\mathrm{HOMO}}$.

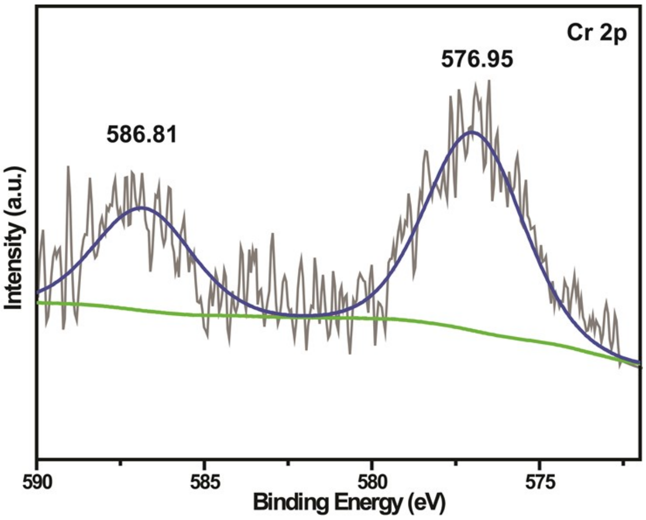

Fig. S7 The XPS spectrum of Cr 2p after photoreduction by PYE-COF.

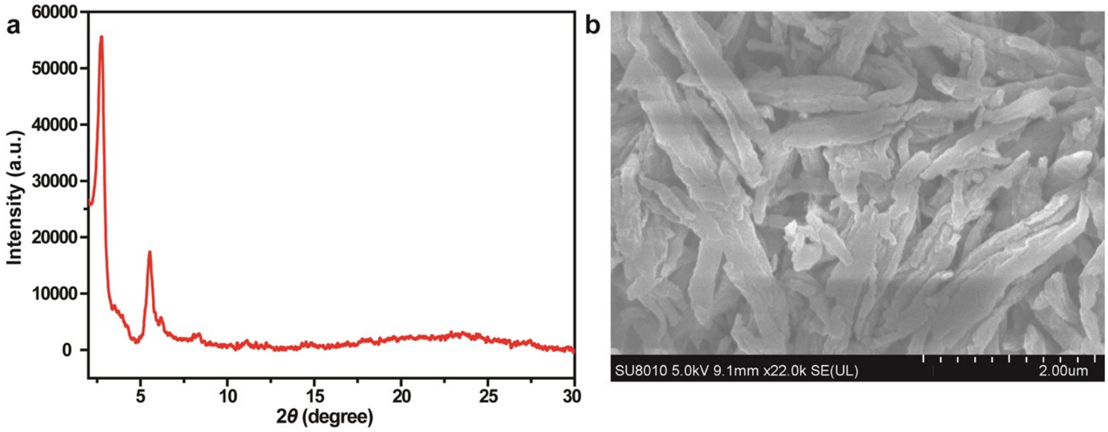

Fig. S8 The PXRD pattern (a) and SEM image of PYE-COF after 5 regeneration-photoreduction cycles.

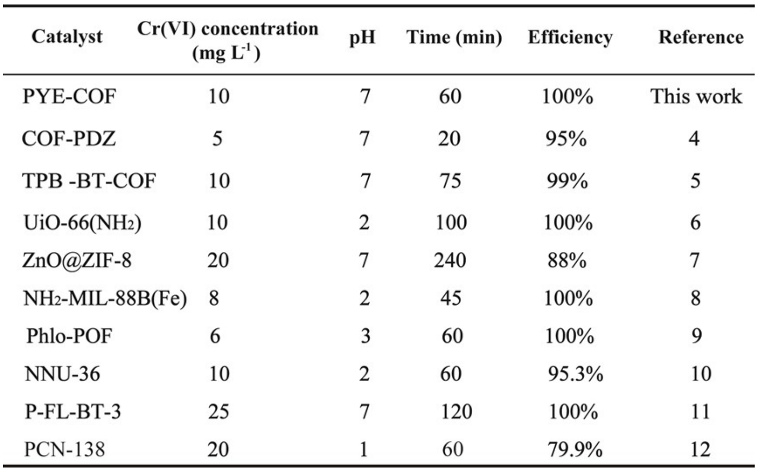

Catalyst	Cr(VI) concentration ($mg L^{-1}$)	pH	Time (min)	Efficiency	Reference
PYE-COF	10	7	60	100%	This work
COF-PDZ	5	7	20	95%	4
TPB -BT-COF	10	7	75	99%	5
UiO-66(NH_2)	10	2	100	100%	6
ZnO@ZIF-8	20	7	240	88%	7
NH_2-MIL-88B(Fe)	8	2	45	100%	8
Phlo-POF	6	3	60	100%	9
NNU-36	10	2	60	95.3%	10
P-FL-BT-3	25	7	120	100%	11
PCN-138	20	1	60	79.9%	12

Tab. S1 The comparison of photocatalytic Cr(VI) reduction efficiency by porous materials.

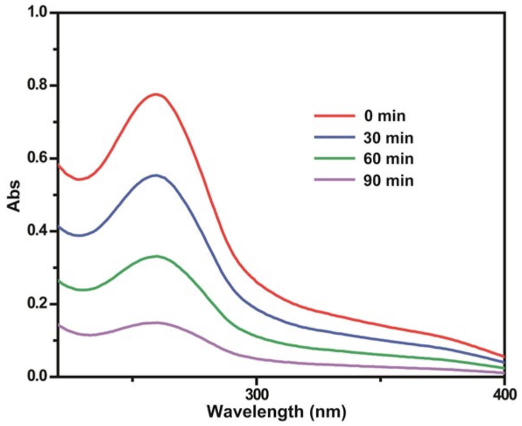

Fig. S9 Detection of $O_2^{\bullet -}$ by NBT.

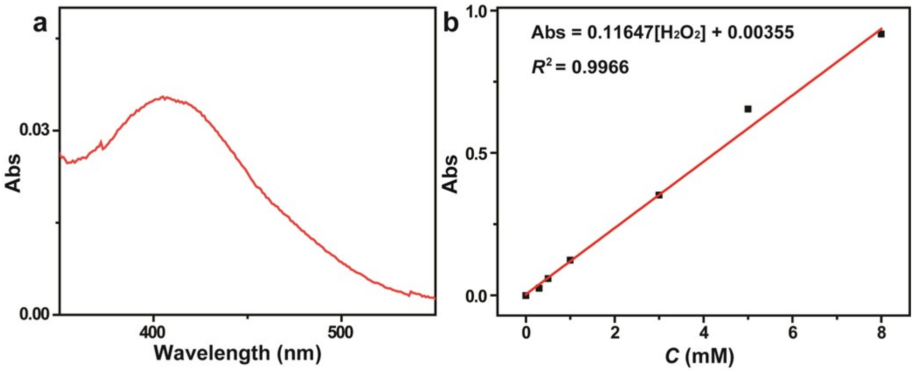

Fig. S10 Detection of H_2O_2 in PYE-COF system after irradiation for 2 h by Titanium sulfate colorimetric method.

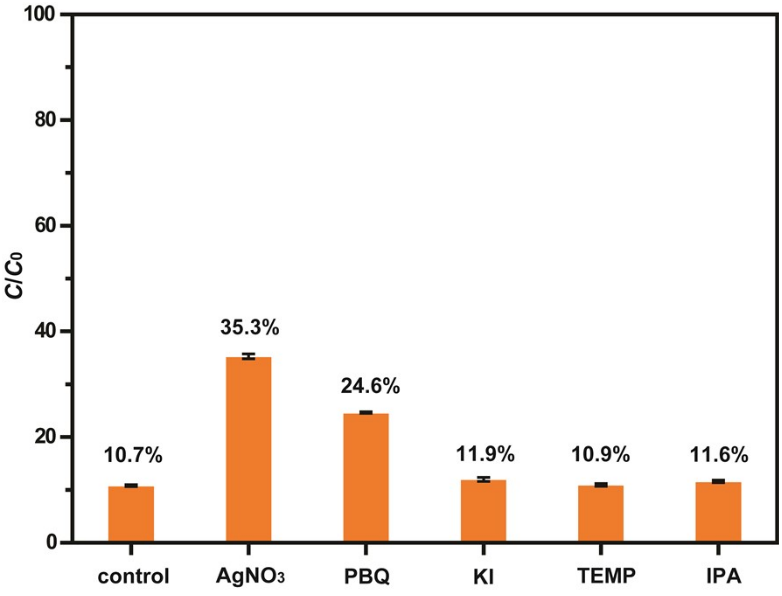

Fig. S11 Photocatalytic performance of Cr(VI) reduction by PYE-COF after irradiation at 40 min with addition of different sacrificial agents, like $AgNO_3$, PBQ, KI, TEMP and IP (0.1 mM).

$\text{PYE-COF} + h\nu \longrightarrow \text{PYE-COF}(e^-) + \text{PYE-COF}(h^+)$	S1
$CrO_4^{2-} + 3\text{PYE-COF}(e^-) + 4H_2O \longrightarrow Cr(OH)_3 + 5OH^- + 3\text{PYE-COF}$	S2
$O_2 + \text{PYE-COF}(e^-) \longrightarrow O_2^{\cdot-} + \text{PYE-COF}$	S3
$CrO_4^{2-} + O_2^{\cdot-} + 3H_2O \longrightarrow Cr(OH)_3 + 3OH^- + 3/2\,O_2$	S4
$\text{PYE-COF}(e^-) + O_2^{\cdot-} + 2H^+ \longrightarrow H_2O_2$	S5
$H_2O_2 \longrightarrow 2\cdot OH$	S6

Tab. S2 The possible mechanism and related equations of photocatalytic Cr(VI) reduction by PYE-COF.

4. References

1 Z. P. Li, S. J. Han, C. Z. Li, P. P. Shao, H. Xia, H. Li, X. Chen, X. Feng and X. M. Liu, *J. Mater. Chem. A*, 2020, **8**, 8706-8715.

2 S. Ghosh, A. Nakada, M. A. Springer, T. Kawaguchi, K. Suzuki, H. Kaji, I. Baburin, A. Kuc, T. Heine, H. Suzuki, R. Abe and S. Seki, *J. Am. Chem. Soc.*, 2020, **142**, 9752-9762.

3 E. Q. Jin, Z. A. Lan, Q. H. Jiang, K. Y. Geng, G. S. Li, X. C. Wang and D. L. Jiang, *Chem*, 2019, **5**, 1632-1647.

4 W.-B. Chen, Z.-F. Yang, Z. Xie, Y.-S. Li, X. Yu, F.-L. Lu and L. Chen, *J. Mater. Chem. A*, 2019, **7**, 998-1004.

5 F. Y. Liu, Z. Y. Ma, Y. C. Deng, M. Wang, P. Zhou, W. Liu, S. J. Guo, M. P. Tong and D. Ma, *Environ. Sci. Technol.*, 2021, **55**, 5371-5381.

6 L. Shen, R. Liang, M. Luo, F. Jing and L. Wu, *Phys. Chem. Chem. Phys.*, 2015, **17**, 117-121.

7 X.-B. Wang, J. Liu, S. Leong, X.-C. Lin, J. Wei, B. Kong, Y.-F. Xu, Z.-X. Low, J.-F. Yao and H.-T. Wang, *ACS Appl. Mater. Interfaces*, 2016, **8**, 9080-9087.

8 L. Shi, T. Wang, H.-B. Zhang, K. Chang, X.-G. Meng, H.-M. Liu and J.-H. Ye, *Adv. Sci.*, 2015, **2**, 1500006.

9 V. Kostas, M. Baikousi, K. Dimos, K. C. Vasilopoulos, I. Koutselas and M. A. Karakassides, *J. Phys. Chem. C*, 2017, **121**, 7303-7311.

10 S. Ghasimi, S. Prescher, Z. J. Wang, K. Landfester, J. Yuan and K. A. Zhang, *Angew. Chem. Int. Ed.*, 2015, **54**, 14549-14553.

11 H. Zhao, Q. Xia, H. Xing, D. Chen and H. Wang, *ACS Sustainable Chem. Eng.*, 2017, **5**, 4449-4456.

12 W.-H. Liu, Z.-F. Guo, Z. Jin, D.-S. Chen, T. Lu, P.-Y. Jia and H.-Z. Xing, *Catal. Sci. Technol.*, 2022, **12**, 2176-2183.